

RESEARCH PAPER

ASKAP EMU Radio Detection of the Reflection Nebula VdB-80 in the Monoceros Crossbones Filamentary Structure

A. C. Bradley,¹ Z. J. Smeaton,¹ N. F. H. Tothill,¹ M. D. Filipović,¹ W. Becker,^{2,3} A. M. Hopkins,⁴ B. S. Koribalski,^{5,1} S. Lazarević,^{1,5,6} D. Leahy,⁷ G. Rowell,⁸ V. Velović,¹ and D. Urošević⁹¹Western Sydney University, Locked Bag 1797, Penrith South DC, NSW 2751, Australia²Max-Planck Institut für extraterrestrische Physik, Gießenbachstraße 1, 85748 Garching, Germany³Max-Planck-Institut für Radioastronomie, Auf dem Hügel 69, 53121 Bonn, Germany⁴School of Mathematical and Physical Sciences, 12 Wally's Walk, Macquarie University, NSW 2109, Australia⁵Australia Telescope National Facility, CSIRO, Space and Astronomy, PO Box 76, Epping, NSW 1710, Australia⁶Astronomical Observatory, Volgina 7, 11060 Belgrade, Serbia⁷Dept. of Physics and Astronomy, University of Calgary, Calgary, AB, T2N 1N4, Canada⁸School of Physics, Chemistry and Earth Sciences, The University of Adelaide, Adelaide 5005, Australia⁹Department of Astronomy, Faculty of Mathematics, University of Belgrade, Studentski trg 16, 11000 Belgrade, Serbia

Author for correspondence: A. C. Bradley, Email: 20295208@student.westernsydney.edu.au.

Abstract

We present a new radio detection from the Australian Square Kilometre Array Pathfinder (ASKAP) Evolutionary Map of the Universe (EMU) survey associated with the Reflection Nebula (RN) VdB-80. The radio detection is determined to be a previously unidentified HII region, now named *Lagotis*. The RN is located towards Monoceros, centred in the molecular cloud feature known as the ‘Crossbones’. The 944MHz EMU image shows a roughly semicircular HII region with an integrated flux density of 30.2 ± 0.3 mJy. The HII region is also seen at 1.4 GHz by NRAO VLA Sky Survey (NVSS), yielding an estimated spectral index of 0.65 ± 0.51 , consistent with thermal radio emission. *Gaia* Data Release 3 (DR3) and Two Micron All Sky Survey (2MASS) data give a distance to the stars associated with the HII region of ~ 960 pc. This implies a size of $0.76 \times 0.68 (\pm 0.09)$ pc for the HII region. We derive an HII region electron density of the bright radio feature to be 26 cm^{-3} , requiring a Lyman-alpha photon flux of $10^{45.6} \text{ s}^{-1}$, which is consistent with the expected Lyman flux of HD 46060, the B2 II type star which is the likely ionising star of the region. The derived distance to this region implies that the Crossbones feature is a superposition of two filamentary clouds, with *Lagotis* embedded in the far cloud.

Keywords: ISM: nebulae, ISM: HII region, ISM: clouds, ISM: molecules, proper motions, stars: distances

1. Introduction

Reflection Nebulae (RNe) are diffuse clouds of gas and dust typically associated with star-forming regions. These RNe are illuminated by young stars and may be accompanied by emission nebulae (Mueller & Graham, 2000; Eiermann et al., 2024). These nebulae are prominent in visible wavelengths, but the visible emission of a RN may be obstructed by dark molecular gas and dust, so the full extent is often better seen in near-infrared (Whitcomb et al., 1981) and far-infrared (Sellgren, 1984) wavelengths.

VdB-80 (also known as [RK68]–59), is a known Galactic RN in the constellation Monoceros, below the Galactic plane at $l = 219^\circ 26$, $b = -8^\circ 93$ (RA(J2000) $\sim 06^{\text{h}} 31^{\text{m}}$, DEC(J2000) $\sim -9^\circ 39'$, van den Bergh, 1966; Rozhkovskij & Kurchakov, 1968; Magakian, 2003).

HII regions are typically associated with sites of early star formation or young stellar clusters embedded in molecular clouds and are comprised of ionised hydrogen (Dyson & Williams, 1997). Ahumada et al. (2001) did not see any signs of an HII region towards VdB-80 in their optical spectra. Nonetheless, we identify radio emission detected by ASKAP as an HII re-

gion that we name ‘*Lagotis*’^a, associated with a stellar cluster in the ‘Crossbones’ molecular cloud, and it is proposed that the star HD 46060 is the centre of both RN and HII region.

The Crossbones is a filamentary cloud structure located within the Mon R2 complex, first characterised by Maddalena et al. (1986), potentially related to the Orion-Eridanus superbubble (Lee & Chen, 2009). This ‘X’ shaped structure is an active star-forming region, with VdB-80 bordering the cloud near to its centre. The structure is most clear in maps of the ($J = 1-0$) rotational transition of ^{12}CO (Dame et al., 1987; Ghosh et al., 2024).

The Australian Square Kilometre Array Pathfinder (ASKAP) (Hotan et al., 2021) Evolutionary Map of the Universe (EMU) (Norris et al., 2011, 2021, Hopkins et al., PASA, submitted.) survey has provided new radio-continuum observations of this region with improved sensitivity compared to any previous radio-continuum surveys. Higher sensitivity has allowed for the first reliable detection of radio-continuum emission toward VdB-80. This new radio detection allows us to estimate properties of the RN that confirm the presence of a HII region, as well as confirming HD 46060’s role as the star responsible for creating both features.

^aNamed after the Australian Greater Bilby (see section 3.4).

This radio detection demonstrates the ability of the newest generation of radio surveys, such as EMU, to detect new low surface-brightness emission. This has been demonstrated in several new discoveries, such as supernova remnants G181.1–9.5 (Kothés *et al.*, 2017), J0624–6948 (Filipović *et al.*, 2022), G288.8–6.3 (Ancora; Filipović *et al.*, 2023; Burger–Scheidlin *et al.*, 2024), G121.1–1.9 (Khabibullin *et al.*, 2023), G308.7+1.4 (Raspberry; Lazarević *et al.*, 2024a), G312.6+ 2.8 (Unicycle; Smeaton *et al.*, 2024), and a pulsar wind nebula (Potoroo; Lazarević *et al.*, 2024b).

The paper is structured as follows: Section 2 outlines the data used, including radio, optical, and infrared data, both new and archival. Section 3 provides analysis and interpretation of Lagotis, this includes distance, size, emission properties and the context of the RN within the Crossbones filaments. Section 4 provides a brief summary of our results and interpretation of Lagotis.

2. Data

2.1 Radio observations

2.1.1 ASKAP

The radio emission associated with VdB-80 was discovered in the ASKAP EMU (AS201) survey. Lagotis appears in two separate EMU observations: Scheduling Block SB59692 observed tile EMU_0626–09A on 2024 March 02, and SB61077 observed tile EMU_0626–09B on 2024 April 13. Both observations were taken at 943.5 MHz with a bandwidth of 288 MHz. The data were reduced using the standard ASKAP pipeline, ASKAPSoft, using multi-frequency synthesis imaging, multi-scale cleaning, self-calibration and convolution to a common beam size (Guzman *et al.*, 2019).

We merged the two images using Multichannel image reconstruction, image analysis and display (MIRIAD) (Sault *et al.*, 1995) task IMCOMB. This merges the images together while applying weighting in the overlapped region to minimise rms noise. SB59692 had significantly more interference from a nearby bright star, and so the weighting ratio of 1:1.5, for SB59692:SB61077, was used to produce the best image. The resulting Stokes I image (Figure 1) has a restored beam size of $15 \times 15''$ and a local rms noise of $\sim 20 \mu\text{Jy beam}^{-1}$. There is no corresponding Stokes V emission.

2.1.2 NVSS

The NRAO VLA Sky Survey (NVSS) covers the entire sky north of -40° (Condon *et al.*, 1998), at 1.4 GHz in the radio continuum, with bandwidth 50 MHz. The Lagotis HII region is also present in this survey, which is used in section 3.1 to obtain characteristics of the RN in radio wavelengths. The NVSS image used has a resolution of $45'' \times 45''$ and a measured local rms noise of $\sim 40 \mu\text{Jy beam}^{-1}$.

2.1.3 CO data

The Crossbones cloud was first observed by Maddalena *et al.* (1986) as part of the Columbia CO survey of the galaxy (Dame *et al.*, 1987). Newer ^{12}CO ($J = 1 \rightarrow 0$) maps of the

Galaxy have been derived from the broadband millimetre-wave maps obtained by the *Planck* satellite (Ghosh *et al.*, 2024).

2.2 Optical observations

van den Bergh (1966) identified HD 46060 as the illuminating star of the RN, noting that it is “in a small compact clustering which includes BD -9° 1497.” Orellana *et al.* (2015) used the UCAC4 astrometric catalogue to identify 8 cluster members of the 23 proposed by Bonatto & Bica (2009).

2.2.1 Gaia

Gaia data for 5 stars that appear to lie within the radio-continuum emission were taken from the *Gaia* Data Release 3 (DR3) (Gaia Collaboration *et al.*, 2016, 2023) catalogue. These values, as well as derived distances, are reported in Table 1. Three of these stars are also listed by Orellana *et al.* (2015); the proper motions are fairly similar, except for UCAC4 402-013691 — Orellana *et al.* do not consider it to be a cluster member, but the *Gaia* proper motion (PM) measurement are much closer to the cluster average.

2.3 Infrared observations

2.3.1 2MASS

Data were collected from Two Micron All Sky Survey (2MASS) (Skrutskie *et al.*, 2006) and used in Section 3.2 to determine accurate distance estimates to the VdB-80, as well as confirming the distance association to the Lagotis HII region. The 2MASS All Sky Catalogue of point sources provides the magnitudes of the RN associated stars in the J, H and K_s ($1.25 \mu\text{m}$, $1.65 \mu\text{m}$ and $2.17 \mu\text{m}$) infrared bands. To verify the association of the RN and the HII region, these magnitudes, as well as a 2MASS J–H/H– K_s extinction map from Froebrich *et al.* (2007), were used to determine stellar position and dust extinction values.

2.3.2 WISE

The Wide-Field Infrared Survey Explorer (WISE) is an all-sky survey in near- and mid-infrared (Wright *et al.*, 2010). Observations were taken in four bands, W1, W2, W3, and W4 with wavelengths $3.4 \mu\text{m}$, $4.6 \mu\text{m}$, $12 \mu\text{m}$ and $22 \mu\text{m}$. The W3 and W4 bands are used with EMU data (Figure 2) to trace the mid-infrared emitting gas and dust that shows the full extent of the RN (Filipović & Tothill, 2021a) at wavelengths other than optical.

2.3.3 AKARI

The *AKARI* far-infrared All-Sky Survey (Doi *et al.*, 2015) comprises four far-infrared bands (65 , 90 , 140 and $160 \mu\text{m}$). *AKARI* data show the gas and dust shroud surrounding the Lagotis HII region and VdB-80 (Figure 3), and are used in conjunction with optical and radio images to create an RGB composite (Figure 4). *AKARI* survey data are useful for mapping the local area surrounding VdB-80, as well as the broader context of the Crossbones filaments.

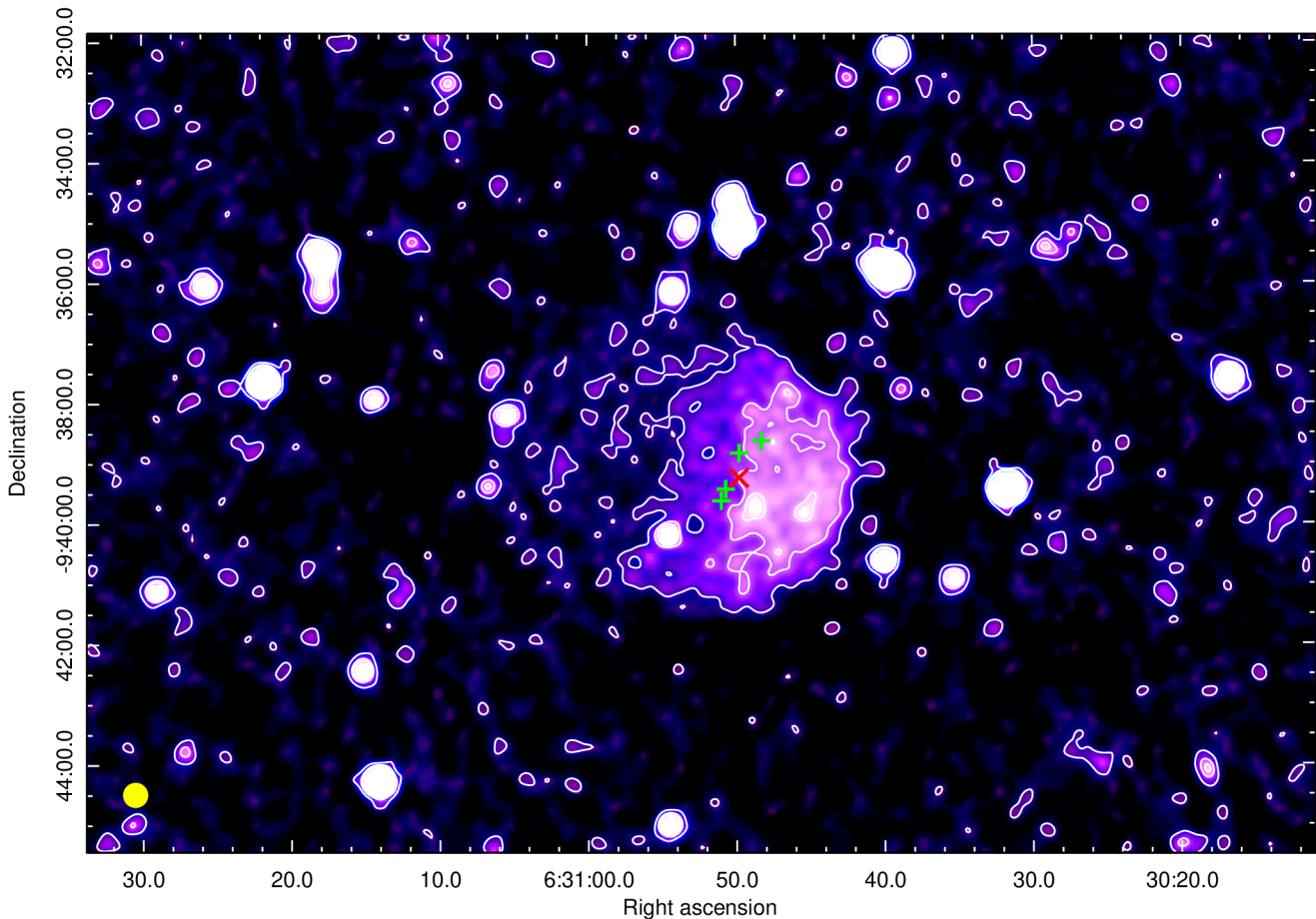


Figure 1. EMU radio-continuum image of Lagotis and VdB-80 at 944 MHz. Local RMS noise is $20 \mu\text{Jy beam}^{-1}$, and contours are at levels of 3, 10 and 15σ . The image resolution is $15 \times 15''$, represented with the yellow circle in the bottom left corner. The red ‘X’ denotes the star HD 46060, and the green crosses denote the other stars in the cluster (see Table 1).

3. Results and Discussion

3.1 VdB-80 Radio-continuum Association

Lagotis, the VdB-80-associated radio-continuum emission detected with EMU is a roughly semi-circular feature with brighter emission in the western part (Figure 1). It can be fitted by an ellipse with size $2'.7 \times 2'.4$, centred at RA(J2000) $6^{\text{h}}30^{\text{m}}53.5^{\text{s}}$ and Dec(J2000) $9^{\circ}39'08''.6$. The whole Lagotis structure has an integrated flux density of $30.2 \pm 3.1 \text{ mJy}$.^b The western side of the feature appears much brighter than the eastern, with integrated flux densities of $25.6 \pm 2.6 \text{ mJy}$ and $4.6 \pm 0.5 \text{ mJy}$.

Lagotis is detected in the NVSS survey at 1.4 GHz under the name NVSS 063048-094007 (Condon et al., 1998). Whilst this has been catalogued in NVSS, there has been no study regarding this emission as an HII region. The radio emission at 1.4 GHz has a measured flux of $39.1 \pm 3.9 \text{ mJy}$, and so a spectral index can be estimated, following the spectral index definition $S \propto \nu^\alpha$ (Filipović & Tothill, 2021b). Convolution of the EMU data to the same resolution as NVSS (beam size = $45 \times 45''$, pixel size = $10 \times 10''$) gives a spectral index of 0.7 ± 0.5 , a fairly flat spectrum which is indicative of thermal radio emission. This spectral index estimate allows us to estimate a surface brightness

value of $\Sigma_{1\text{GHz}} \sim 7.3 \times 10^{-22} \text{ W m}^{-2} \text{ Hz}^{-1} \text{ sr}^{-1}$; assuming a distance of 960 pc, this gives a luminosity at 1 GHz of $\sim 3.6 \times 10^{12} \text{ W Hz}^{-1}$. The approximately circular radio emission fits well inside the far-infrared emitting shell of gas and dust, as shown in Figure 4.

3.2 Distance and Size

Gaia parallaxes of the young stars associated with the RN VdB-80 and in the centre of the Lagotis HII region (Table 1) are taken from *Gaia* DR3 (Gaia Collaboration et al., 2016, 2023). The derived distances range from 914 to 1127 pc. Since this range is much larger than the size of the stellar association^c, we treat all stars as lying at an error-weighted average distance of 960 pc, with an uncertainty of about 100 pc.

Wilson et al. (2005) estimated a distance to the Crossbones (and by extension Lagotis and VdB-80) of 465 pc using Hipparcos parallaxes, significantly closer than the distance we derive using *Gaia* data — this disparity is considered further in section 3.3. We take the value of $960 \pm 100 \text{ pc}$ to be accurate as *Gaia* parallax is more reliable than the Hipparcos parallax used for the closer distance derivation (Al-Wardat et al., 2021).

^bWe measure the flux density and error following the same procedure as in Filipović et al. (2022) and Filipović et al. (2023).

^cThe young stars spread over about an arcminute on the sky, $<1 \text{ pc}$ at $\sim 1 \text{ kpc}$.

Table 1. *Gaia* properties of stars within VdB-80. Columns [2] and [3] are FK5 (J2000) right ascension and declination positions. Column [4] is parallax and its associated error in milliarcseconds. Column [5] is distance and its associated error, as calculated from column [4], in parsecs. Column [6] is the right ascension proper motion, and column [7] is the declination proper motion in milliarcseconds per year.

[1] Star Name	[2] RA (J2000) (h:m:s)	[3] DEC (J2000) (d:m:s)	[4] $p \pm \Delta p$ (mas)	[5] $d \pm \Delta d$ (pc)	[6] μ (RA) (mas yr ⁻¹)	[7] μ (DEC)
HD 46060; NSV 2998; UCAC4 402-013688	06:30:49.8	-09:39:14.8	1.0711±0.0220	933±19	-3.526	0.154
BD-09 1497	06:30:48.3	-09:38:38.0	1.0532±0.0191	949±18	-3.428	0.226
UCAC4 402-013691	06:30:50.7	-09:39:26.1	1.0261±0.0184	975±18	-3.520	0.730
UCAC4 402-013693	06:30:51.0	-09:39:37.7	1.0430±0.0238	959±22	-3.190	0.270
Gaia DR3 3002950320576187904	06:30:49.8	-09:38:50.1	0.9483±0.0645	1055±72	-3.210	0.199

Within the region of the radio-continuum emission, there are around 150 identified stars (Gaia Collaboration et al., 2016, 2023) with varying magnitudes and distances. The cluster of stars proposed to be associated with the VdB-80 RN includes 12 of these, of which we use a subset of five stars, including HD 46060 (Table 1); these appear to be central to the radio feature. These stars were chosen based on their central location in the radio-continuum feature, and within 40 arcseconds of the proposed host star; HD 46060 (see section 3.4.). The distance is taken to be the error-weighted average distance of the five stars, which puts VdB-80 at 960 ± 100 pc. From the radio angular size of $2'.7 \times 2'.4$, we estimate the physical size to be $0.75 \times 0.67 (\pm 0.09)$ pc.

2MASS extinction data show that the stellar cluster and VdB-80 are in the same plane and share a common distance. Table 2 shows near-IR 2MASS brightnesses for the same stars, along with colour excess ($J - H/H - K_s$) and visual extinction A_V , calculated using formulae from Froebrich & del Burgo (2006) and Froebrich et al. (2007). The extinction values show a few magnitudes' reddening of the stars, similar to those found towards the Crossbones (Froebrich et al., 2007), indicating that they are embedded in the cloud. There is a distinct correlation between 2MASS extinction and *Gaia* distance (Tables 1 & 2): This suggests that HD 46060 is towards the front of the cloud (or may have cleared enough material to have lower extinction), while the other stars are more deeply embedded in the cloud behind HD 46060. The embedding of the stars underlines their association with the Crossbones cloud, and implies that the *Gaia* distance can be used for the cloud.

3.3 Crossbones

The 'Crossbones' in Monoceros is an 'X'-shaped molecular cloud structure prominent in both ¹²CO and ¹³CO maps (Maddalena et al., 1986; Kim et al., 2004). It was originally identified as part of the Orion-Monoceros cloud complex by Maddalena et al.: The Orion A and B clouds run approximately N-S, with northern and southern filaments running E-W. Crossbones appears to be part of the S filament, near where the Monoceros R2 (Mon R2) molecular cloud overlaps with the filament. At a distance of 800–900 pc Mon R2 lies far behind the Orion clouds (400–500 pc), and is not associated. Crossbones has been taken to be a spatially coherent

structure because the velocities of its parts appear coherent. Maddalena et al., noting that the stars associated with VdB-80 had estimated distances ~ 800 pc, suggested that the entire southern filament might be associated with Mon R2, rather than Orion. Wilson et al. (2005) derived a distance of ~ 460 pc to the southern filament from *Hipparcos* stellar parallaxes.

The Lagotis HII region is embedded at the edge of the NE-SW arm of the Crossbones, close to the point where the arms cross (Figure 3). This can be seen in the far-IR images, in which a larger far-IR bright region envelops the HII region, while the CO 1–0 emission has a cavity in the same place. The pressure of the HII region and the UV flux of its star are excavating the cavity in the molecular cloud, and the dust around the cavity is being heated up to generate the far-IR emission (Figure 3). The calculated Lyman flux of HD 46060 (see section 3.4.) is consistent with the HII region observed; this supports the argument that HD46060 and its neighbours not only illuminate VdB-80, but also power the Lagotis HII region. Hence, the distance of these stars is the likely distance of this molecular gas structure.

The most likely interpretation of the data is that Crossbones is not a contiguous structure, but a superposition of a NE-SW filamentary cloud and the southern filament of the Orion-Monoceros cloud complex. The population of YSOs found by Lee & Chen (2009) towards Crossbones are largely found towards the NE-SW arm, which also appears brighter in CO and far-IR. We therefore suggest that the NE-SW arm of Crossbones is a dense star-forming cloud at the distance of (and possibly associated with) Mon R2; the SE-NW arm of Crossbones is simply part of the less dense southern Orion filament. The only evidence against this interpretation is the lack of velocity discontinuity between the two arms.

From the CO 1–0 data (Ghosh et al., 2024), we estimate an excitation temperature towards Lagotis of 12 K, compared to the 17 K found towards Mon R2 (Pokhrel et al., 2016). Considering the beam dilution in the rather large *Planck* beam, these temperature values are reasonably consistent.

3.4 The Stellar Cluster and the HII Region

The *Gaia* proper motions of the main stars in the stellar cluster (Table 1) suggest that the cluster is moving into the Crossbones filaments near the centre (Figure 3). Based on this

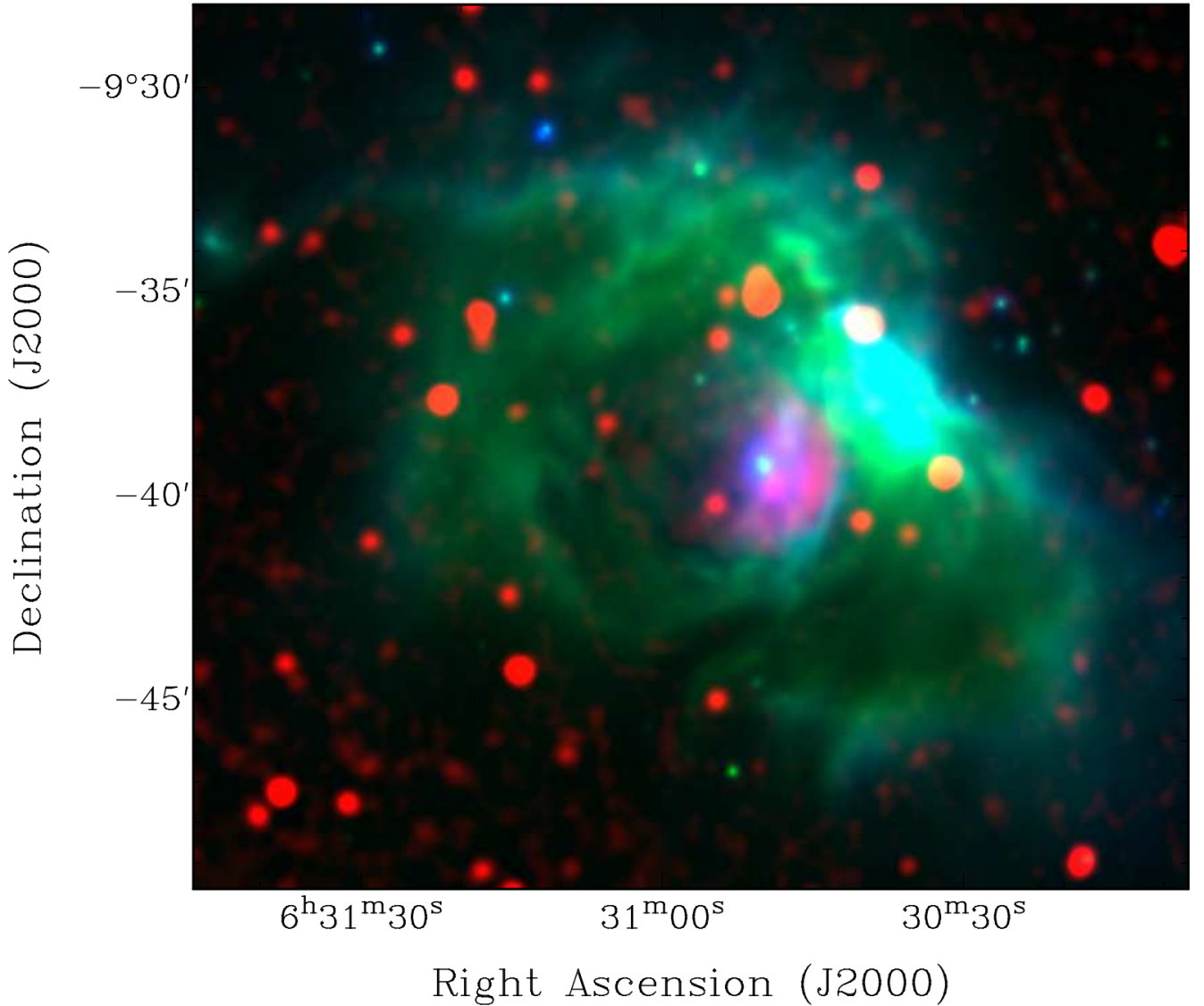


Figure 2. An RGB image tracing the near-infrared emission of VdB-80, where red is the EMU tile SB61077 (smoothed to a $25''$ resolution) at 943.5 GHz, green is the WISE W3 band ($12\mu\text{m}$) and blue is the WISE W4 band ($22\mu\text{m}$).

movement, we give the HII region the designation ‘Lagotis’, as the stars are moving, or ‘burrowing’ into the HII region and the molecular cloud^d.

In the larger scope of the stellar cluster, there is a large population of stars at a similar distance (~ 1 kpc); the majority of stars in this cluster have similar proper motion profiles to the Lagotis stars (Table 1). Due to its central location and brightness, we propose that HD 46060 is the main driver of the HII region. This star is the brightest in the central cluster and has generally been associated with the RN itself. The distance from HD 46060 to the edge of the bright emission is 0.49 pc, and we take this to be the radius of the HII region. We also assume the electron temperature of the HII region to be 10^4 K. Using the equations in Dyson & Williams (1997)

^dLagotis comes from the Latin *Macrotis Lagotis*, the Australian Greater Bilby, <https://australian.museum/learn/animals/mammals/greater-bilby/>.

and Schmiedeke et al. (2016), we derive an electron density of 26 cm^{-3} , which can then be used to estimate an ionising flux of $10^{45.6}\text{ s}^{-1}$.

HD 46060 has been variously classified as a spectral type of B8 (van den Bergh, 1966; Ochsenbein, 1980), B3ne (Racine, 1968), B2 II (Houk & Swift, 2000; Kharchenko, 2001; Anderson & Francis, 2012) and B2 III–IV (Aveni & Hunter, 1972). Based on the most recent results, we adopt a spectral type of B2 II. HD 46060 is about 4.5 ± 1.5 Myr old, (Ahumada et al., 2001), so its ionising flux is expected to be higher than the zero-age-main-sequence (ZAMS) value of $10^{44.7}\text{ s}^{-1}$. Panagia (1973) gives a range of ionising fluxes for B2 I–III that is consistent with our estimated ionising flux of $10^{45.6}\text{ s}^{-1}$.

We therefore put forward a self-consistent interpretation in which HD 46060 is a B2 II star with sufficient ionising flux to power the Lagotis HII region with radius 0.49 pc and electron

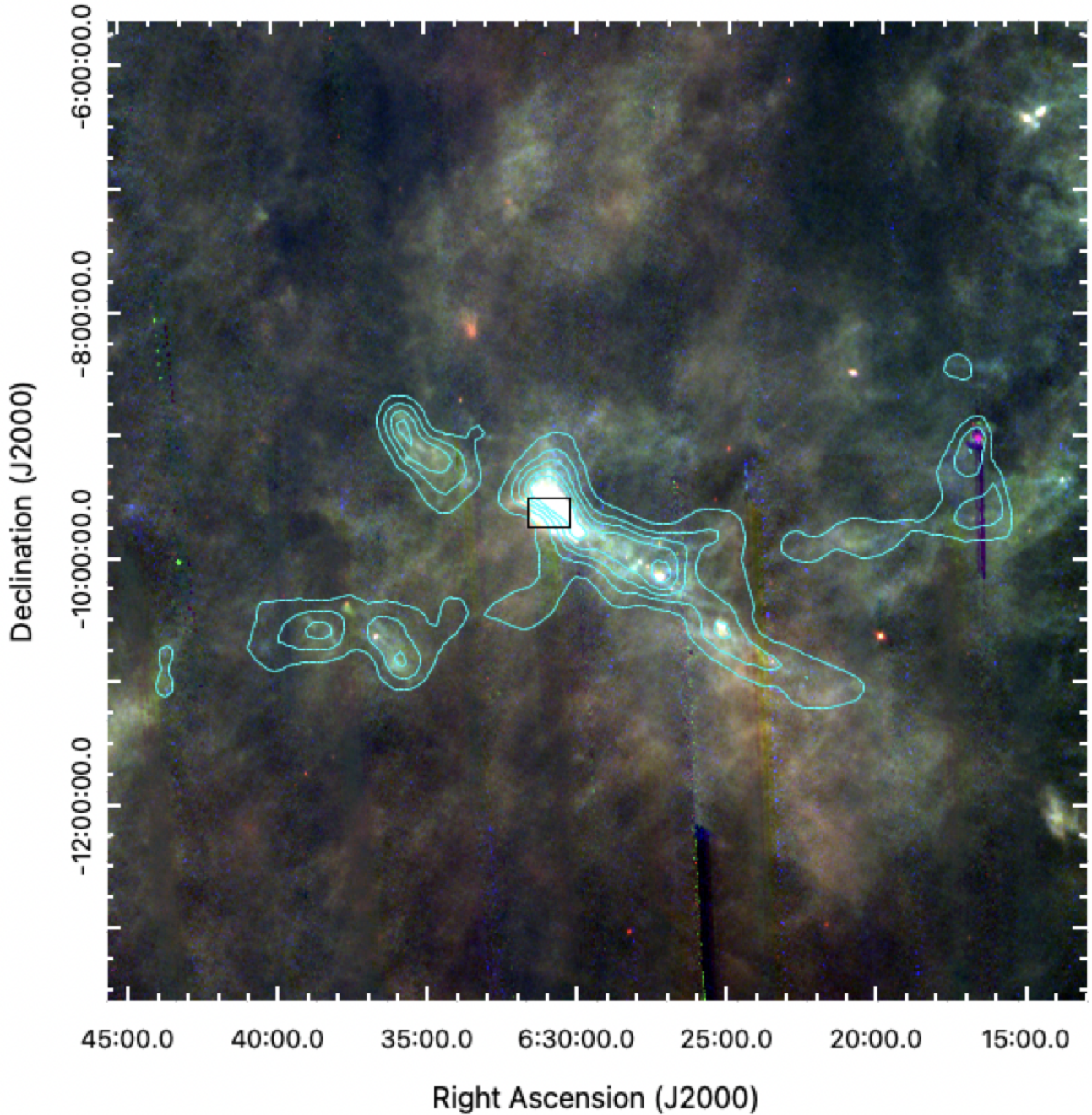


Figure 3. RGB composite image of the Crossbones filaments in far-infrared. Red is *AKARI* N160 (160 μm band), green is *AKARI* WIDE-L (140 μm band) and blue is *AKARI* WIDE-S (90 μm band). Contours in cyan are generated from the ^{12}CO ($J=1-0$) map provided by Ghosh *et al.* (2024). The black square in the image represents the size of Figure 1, Lagotis corresponds to the bright emission in far-infrared. Fragmented vertical lines present in the image are artefacts from *AKARI* observations.

density 26 cm^{-3} . This gives rise to thermal radio continuum emission, consistent with the estimated flux density.

Because VdB-80 sits on the edge of the cloud, there may be a champagne flow (Comeron, 1997; Immer *et al.*, 2014) from the Lagotis HII region that is not seen in the EMU image, with supersonic movement of ionised gas caused by a steep pressure and density gradient at the edge of the cloud (Bodenheimer *et al.*, 1979). This is consistent with the roughly hemispherical

shape of the HII region, and may be the cause for the dim eastern side of the radio-continuum emission. More sensitive observations at additional frequencies may be able to test this possibility.

4. Conclusion

Sensitive EMU observations have revealed radio-continuum emission at 943.5 MHz toward a known RN, VdB-80 (van den

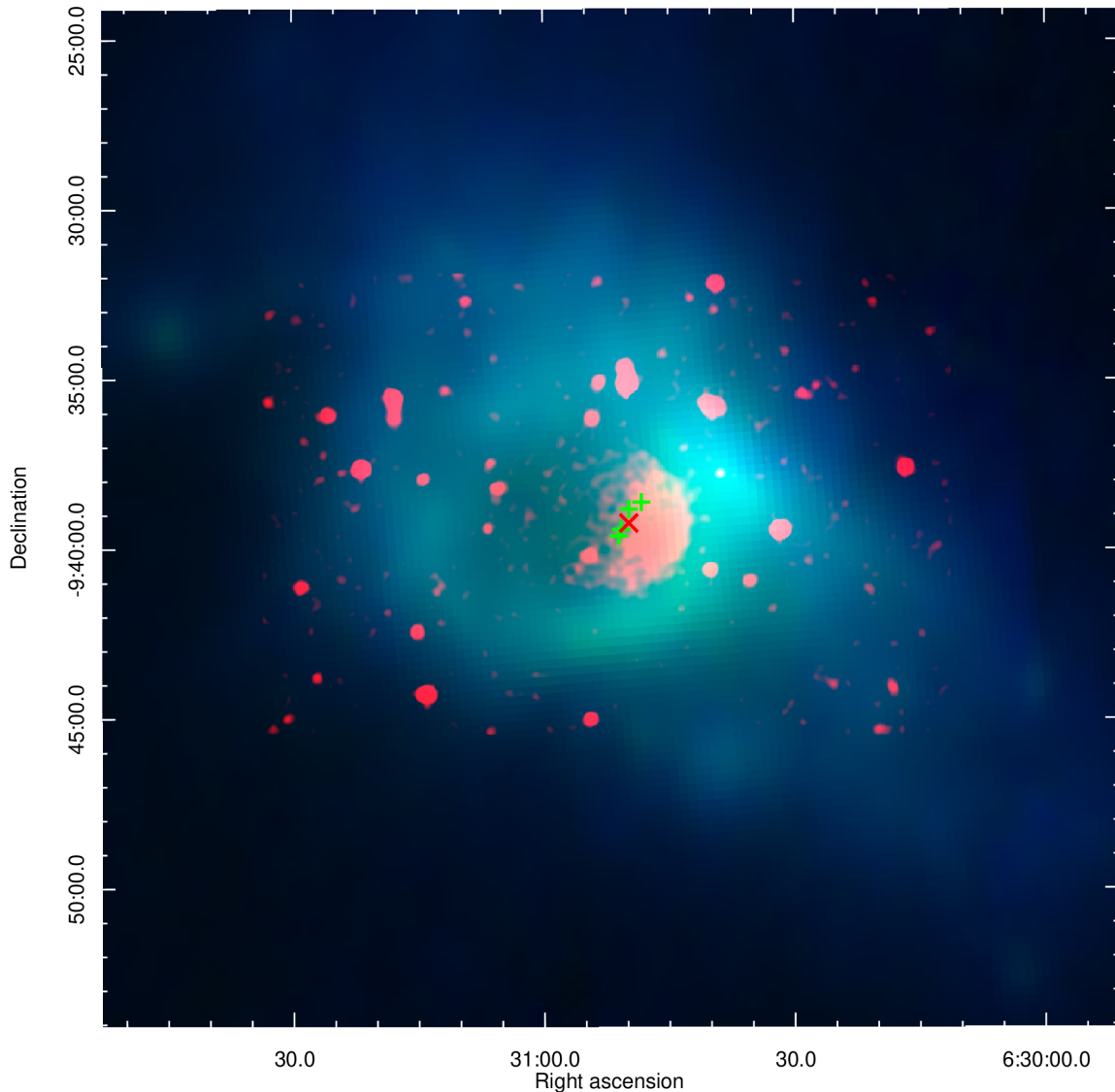


Figure 4. RGB image of Lagotis HII region and VdB-80, where red is the EMU radio image (943.5 MHz), green is an *AKARI* wide-S band (90 μm) image, and blue is an *AKARI* wide-L band (140 μm) image. The red ‘X’ denotes the star HD 46060, and the green crosses denote the other stars in the cluster (Table 1).

Bergh, 1966). This is a unique feature for an object mainly known for its optical properties. The emission — nicknamed *Lagotis* — is measured to be 30.2 ± 0.3 mJy, and is comprised of bright (Western side) and dim (Eastern side) portions with flux densities of 25.6 ± 2.6 mJy and 4.6 ± 0.5 mJy.

The radio-continuum detection is a circular feature with the brighter side pointed inward toward the Crossbones cloud filaments, accompanied by a bright shroud of far-infrared emission and an extended shell of mid-infrared emission (Figures 2 & 4). This indicates heating of the cloud surrounding the RN, which is likely to be a byproduct of a HII region heating up the gas and dust surrounding its shell. This shows that the features associated with the RN and HII region extend much further than shown in visible wavelengths.

VdB-80 and Lagotis are situated at the edge of the Crossbones molecular cloud structure. We find the RN to be at a distance of 960 ± 100 pc based on *Gaia* parallax values for a subset of stars in the stellar cluster association. From this

distance, we estimate the size of the radio emission to be $0.75 \times 0.67 (\pm 0.09)$ pc, and we find that the Crossbones feature is most likely a superposition of two filamentary clouds associated with Orion (in the foreground) and Mon R2 (in the background).

The proper motion (Table 1) of the stellar cluster associated with the RN shows that the cluster is moving toward, and ‘into’ the cloud. The proposed driver of the HII region is HD 46060, a B2 II type star at the center of the stellar cluster, with enough ionising output to power the HII region, with an estimated electron density of 26 cm^{-3} . Irregularities in the radio feature as well as the far-infrared emitting shell may be generated from the other stars in the cluster with unknown spectral types.

Objects with low surface brightness, such as Lagotis, are becoming more prominent in high sensitivity surveys such as EMU. This discovery of the radio-continuum emission associated with an RN and its analysis has indicated that HD 46060 both powers Lagotis and illuminates VdB-80. ASKAP and

Table 2. Near-IR 2MASS JHK_s magnitudes for the five star subset of the stellar cluster; and calculated near-IR colour excess ($J - H/H - K_s$) and visual extinction A_V , derived according to Froebrich & del Burgo (2006). The error in extinction arises from the variation between $J - H$ and $H - K_s$ colours.

Star Name	J	H	K_s	$J-H/H-K_s$	Extinction
HD 46060	8.153	8.134	8.105	0.65	5.34 ± 0.02
BD-09 1497	9.643	9.490	9.378	1.60	6.26 ± 0.11
UCAC4 402-013961	10.808	10.478	10.317	2.00	6.96 ± 0.20
UCAC4 402-013693	10.395	10.297	10.239	1.69	6.79 ± 0.07
Gaia DR3 3002950320576187904	13.702	12.867	12.532	2.50	8.67 ± 0.49

other new-generation telescopes enable future observations and discoveries of RNe with radio-continuum emission.

Acknowledgement

This scientific work uses data obtained from Inyarrimanha Ilgari Bundara / the Murchison Radio-astronomy Observatory. We acknowledge the Wajarri Yamaji People as the Traditional Owners and native title holders of the Observatory site. CSIRO's ASKAP radio telescope is part of the Australia Telescope National Facility (<https://ror.org/05qajvd42>). Operation of ASKAP is funded by the Australian Government with support from the National Collaborative Research Infrastructure Strategy. ASKAP uses the resources of the Pawsey Supercomputing Research Centre. Establishment of ASKAP, Inyarrimanha Ilgari Bundara, the CSIRO Murchison Radio-astronomy Observatory and the Pawsey Supercomputing Research Centre are initiatives of the Australian Government, with support from the Government of Western Australia and the Science and Industry Endowment Fund.

This work has made use of data from the European Space Agency (ESA) mission *Gaia* (<https://www.cosmos.esa.int/gaia>), processed by the *Gaia* Data Processing and Analysis Consortium (DPAC, <https://www.cosmos.esa.int/web/gaia/dpac/consortium>). Funding for the DPAC has been provided by national institutions, in particular the institutions participating in the *Gaia* Multilateral Agreement. This publication makes use of data products from the Two Micron All Sky Survey, which is a joint project of the University of Massachusetts and the Infrared Processing and Analysis Center/California Institute of Technology, funded by the National Aeronautics and Space Administration and the National Science Foundation. This research is based on observations with *AKARI*, a JAXA project with the participation of ESA.

Funding Statement MDF, GR and SL acknowledge Australian Research Council (ARC) funding through grant DP200100784. DU acknowledges the financial support provided by the Ministry of Science, Technological Development and Innovation of the Republic of Serbia through the contract 451-03-66/2024-03/200104 and for support through the joint project of the Serbian Academy of Sciences and Arts and Bulgarian Academy of Sciences “Optical search for Galactic and extragalactic supernova remnants”.

Competing Interests None.

Data Availability Statement EMU data can be accessed through the CSIRO ASKAP Science Data Archive (CASDA) portal: <https://research.csiro.au/casda>. NVSS data can be obtained from the NVSS Postage Stamp Server: <https://www.cv.nrao.edu/nvss/postage.shtml>. All *Gaia* DR3 data are obtained from the *Gaia* Archive website: <https://gea.esac.esa.int/archive/>. Data from the 2MASS Point Source Catalogue are available from the NASA/IPAC Infrared Science Archive (IRSA): <https://irsa.ipac.caltech.edu/Missions/2mass.html>. WISE data is available from the NASA/IPAC Infrared Science Archive (IRSA): <https://irsa.ipac.caltech.edu/Missions/wise.html>. Data from the *AKARI* all-sky survey are available at the NASA/IPAC Infrared Science Archive (IRSA): <https://irsa.ipac.caltech.edu/data/AKARI/>.

References

- Ahumada, A. V., Clariá, J. J., Bica, E., Dutra, C. M., & Torres, M. C. 2001, *Astronomy & Astrophysics*, 377, 845
- Al-Wardat, M. A., Hussein, A. M., Al-Naimiy, H. M., & Barstow, M. A. 2021, *Publications of the Astronomical society of Australia*, 38, e002
- Anderson, E., & Francis, C. 2012, *Astronomy Letters*, 38, 331
- Aveni, A. F., & Hunter, J. H. 1972, *The Astronomical Journal*, 77, 17
- Bodenheimer, P., Tenorio-Tagle, G., & Yorke, H. W. 1979, *The Astrophysical Journal*, 233, 85
- Bonatto, C., & Bica, E. 2009, *MNRAS*, 397, 1915
- Burger-Scheidlin, C., Brose, R., Mackey, J., et al. 2024, *Astronomy & Astrophysics*, 684, A150
- Comeron, F. 1997, *Astronomy & Astrophysics*, 326, 1195
- Condon, J. J., Cotton, W. D., Greisen, E. W., et al. 1998, *The Astronomical Journal*, 115, 1693
- Dame, T. M., Ungerechts, H., Cohen, R. S., et al. 1987, *The Astrophysical Journal*, 322, 706
- Doi, Y., Takita, S., Ootsubo, T., et al. 2015, *Publications of the Astronomical Society of Japan*, 67, 50
- Dyson, J. E., & Williams, D. A. 1997, *The physics of the interstellar medium* (Bristol, Philadelphia, Institute of Physics Pub), doi:10.1201/9780585368115
- Eiermann, J. M., Caputo, M., Lai, T. S. Y., & Witt, A. N. 2024, *Monthly Notices of the Royal Astronomical Society*, 529, 1680
- Filipović, M. D., & Tohill, N. F. H. 2021a, *Multimessenger Astronomy in Practice*, doi:10.1088/2514-3433/ac2256
- . 2021b, *Principles of Multimessenger Astronomy*, doi:10.1088/2514-3433/ac087e
- Filipović, M. D., Payne, J. L., Alsaberi, R. Z. E., et al. 2022, *Monthly Notices of the Royal Astronomical Society*, 512, 265
- Filipović, M. D., Dai, S., Arbutina, B., et al. 2023, *The Astronomical Journal*, 166, 149
- Froeblich, D., & del Burgo, C. 2006, *Monthly Notices of the Royal Astronomical Society*, 369, 1901
- Froeblich, D., Murphy, G. C., Smith, M. D., Walsh, J., & Del Burgo, C. 2007, *Monthly Notices of the Royal Astronomical Society*, 378, 1447

- Gaia Collaboration, Prusti, T., de Bruijne, J. H. J., et al. 2016, *Astronomy & Astrophysics*, 595, A1
- Gaia Collaboration, Vallenari, A., Brown, A. G. A., et al. 2023, *Astronomy & Astrophysics*, 674, A1
- Ghosh, S., Remazeilles, M., & Delabrouille, J. 2024, *Astronomy & Astrophysics*, 688, A54
- Guzman, J., Whiting, M., Voronkov, M., et al. 2019, ASKAPsoft: ASKAP science data processor software, *Astrophysics Source Code Library*, record ascl:1912.003
- Hotan, A. W., Buntun, J. D., Chippendale, A. P., et al. 2021, *Publications of the Astronomical society of Australia*, 38, e009
- Houk, N., & Swift, C. 2000, *VizieR Online Data Catalog: Michigan Catalogue of HD stars, Vol.5 (Houk+, 1999)*, *VizieR On-line Data Catalog: III/214*. Originally published in: Department of Astronomy, University of Michigan, Ann Arbor Michigan (1999)
- Immer, K., Cyganowski, C., Reid, M. J., & Menten, K. M. 2014, *Astronomy & Astrophysics*, 563, A39
- Khabibullin, I. I., Churazov, E. M., Bykov, A. M., Chugai, N. N., & Sunyaev, R. A. 2023, *Monthly Notices of the Royal Astronomical Society*, 521, 5536
- Kharchenko, N. V. 2001, *Kinematika i Fizika Nebesnykh Tel*, 17, 409
- Kim, B. G., Kawamura, A., Yonekura, Y., & Fukui, Y. 2004, *Publications of the Astronomical Society of Japan*, 56, 313
- Kothes, R., Reich, P., Foster, T. J., & Reich, W. 2017, *Astronomy & Astrophysics*, 597, A116
- Lazarević, S., Filipović, M. D., Koribalski, B. S., et al. 2024a, *Research Notes of the American Astronomical Society*, 8, 107
- Lazarević, S., Filipović, M. D., Dai, S., et al. 2024b, *Publications of the Astronomical society of Australia*, 41, e032
- Lee, H.-T., & Chen, W. P. 2009, *The Astrophysical Journal*, 694, 1423
- Maddalena, R. J., Morris, M., Moskowitz, J., & Thaddeus, P. 1986, *The Astrophysical Journal*, 303, 375
- Magakian, T. Y. 2003, *Astronomy & Astrophysics*, 399, 141
- Mueller, K. E., & Graham, J. A. 2000, *Publications of the Astronomical Society of the Pacific*, 112, 1426
- Norris, R. P., Hopkins, A. M., Afonso, J., et al. 2011, *Publications of the Astronomical society of Australia*, 28, 215
- Norris, R. P., Marvil, J., Collier, J. D., et al. 2021, *Publications of the Astronomical society of Australia*, 38, e046
- Ochsenbein, F. 1980, *Bulletin d'Information du Centre de Donnees Stellaires*, 19, 74
- Orellana, R. B., De Biasi, M. S., Paíz, L. G., Bustos Fierro, I. H., & Calderón, J. H. 2015, *New A*, 36, 70
- Panagia, N. 1973, *The Astronomical Journal*, 78, 929
- Pokhrel, R., Gutermuth, R., Ali, B., et al. 2016, *Monthly Notices of the Royal Astronomical Society*, 461, 22
- Racine, R. 1968, *The Astrophysical Journal*, 73, 233
- Rozhkovskij, D. A., & Kurchakov, A. V. 1968, *Trudy Astrofizicheskogo Instituta Alma-Ata*, 11, 3
- Sault, R. J., Teuben, P. J., & Wright, M. C. H. 1995, in *Astronomical Society of the Pacific Conference Series, Vol. 77, Astronomical Data Analysis Software and Systems IV*, ed. R. A. Shaw, H. E. Payne, & J. J. E. Hayes, 433
- Schmiedeke, A., Schilke, P., Möller, T., et al. 2016, *Astronomy & Astrophysics*, 588, A143
- Sellgren, K. 1984, *The Astrophysical Journal*, 277, 623
- Skrutskie, M. F., Cutri, R. M., Stiening, R., et al. 2006, *The Astronomical Journal*, 131, 1163
- Smeaton, Z. J., Filipović, M. D., Koribalski, B. S., et al. 2024, *Research Notes of the American Astronomical Society*, 8, 158
- van den Bergh, S. 1966, *The Astronomical Journal*, 71, 990
- Whitcomb, S. E., Gatley, I., Hildebrand, R. H., et al. 1981, *The Astrophysical Journal*, 246, 416
- Wilson, B. A., Dame, T. M., Masheder, M. R. W., & Thaddeus, P. 2005, *Astronomy & Astrophysics*, 430, 523
- Wright, E. L., Eisenhardt, P. R. M., Mainzer, A. K., et al. 2010, *The Astronomical Journal*, 140, 1868